Virus Research 176 (2013) 199–210

Contents lists available at SciVerse ScienceDirect

Virus Research

journal homepage: www.elsevier.com/locate/virusres

Evidence suggesting that HCV p7 protects E2 glycoprotein from premature degradation during virus production

Ali M. Atoom, Daniel M. Jones, Rodney S. Russell*

Immunology and Infectious Diseases, Faculty of Medicine, Memorial University of Newfoundland, St. John's, Newfoundland, Canada

ARTICLE INFO

Article history:
Received 22 February 2013
Received in revised form 14 June 2013
Accepted 20 June 2013
Available online 28 June 2013

Keywords:
RNA viruses
Flaviviruses
Hepatitis C virus
Virus production
Virus assembly

ABSTRACT

The hepatitis C virus (HCV) genome encodes a 63 amino acid (aa) protein, p7, which is located between the structural and non-structural proteins. p7 localizes to endoplasmic reticulum membranes and is composed of two transmembrane domains (TM1 and TM2) and a cytoplasmic loop. While its exact role is unknown, p7 is crucial for assembly and/or release of infectious virus production in cell culture, as well as infectivity in chimpanzees. The contribution of p7 to the HCV life cycle may result from at least two distinct roles. Firstly, several studies have shown that p7 acts as an ion channel, the functionality of which is critical for infection. Secondly, p7 interacts with NS2 in a manner that may regulate the targeting of other structural proteins during the assembly process. In this study, we observed that mutations in TM1 and the cytoplasmic loop of p7 decreased infectious virus production in a single-cycle virus production assay. Analysis of intra- and extracellular virus titers indicated that p7 functions at a stage prior to generation of infectious particles. These effects were not due to altered RNA replication since no effects on levels of NS3 or NS5A protein were observed, and were not a consequence of altered recruitment of core protein to lipid droplets. Similarly, these mutations seemingly did not prevent nucleocapsid oligomerization. Importantly, we found that an alanine triplet substitution including the two basic residues of the cytoplasmic loop, which is integral to p7 ion channel function, significantly reduced E2 glycoprotein levels. A time course experiment tracking E2 levels indicated that E2 was degraded over time, as opposed to being synthesized in reduced quantities. The results of this study provide strong evidence that one of the functions of p7 is to protect HCV glycoproteins from premature degradation during virion morphogenesis.

1. Introduction

Hepatitis C virus (HCV) infection is a major global health problem with an estimated 123–180 million people infected worldwide, which represents 2–3% of the global population (Shepard et al., 2005; Martins et al., 2011). HCV infection frequently causes chronic liver disease that can progress to cirrhosis and hepatocellular carcinoma. Prior to the recent introduction of direct-acting antivirals in clinics, treated individuals received a combination of pegylated interferon and ribavirin, which is poorly effective and associated with severe side effects (Michaels and Nelson, 2010). Therefore, an alternative therapeutic strategy composed of a multi-targeted, virus-specific approach is required. To realize this potential we must first gain a better understanding of the basic function of some of the more poorly understood viral proteins.

HCV is a small enveloped virus that belongs to the *Hepacivirus* genus within the *Flaviviridae* family. The viral genome is a single-stranded, positive sense RNA molecule of approximately 9.6 kb in length, and encodes approximately 3000 amino acids (aa) (Tellinghuisen et al., 2007; Murray et al., 2008). The viral polypeptide chain is generated following recognition of the viral RNA genome by host cell translation machinery, and is co- and post-translationally processed by host and viral proteases to liberate individual viral gene products (Bartenschlager et al., 2011). The N-terminal region of the generated polyprotein encodes three proteins, namely core and the envelope proteins E1 and E2, which provide structural components of the virus particle (Op De Beeck et al., 2004; McLauchlan, 2009). The C-terminal portion encodes the viral non-structural proteins, including NS3, NS4A, NS4B, NS5A, and NS5B, which are all essential for production of viral RNA, and many of these proteins also play roles in virus assembly (Moradpour et al., 2007; Appel et al., 2008; Ma et al., 2008; Masaki et al., 2008; Jones et al., 2009, 2011; Popescu et al., 2011a,b). The HCV polyprotein also encodes two additional proteins, known as p7 and NS2, that are not

* Corresponding author. Tel.: +1 709 777 8974.
E-mail address: rodney.russell@med.mun.ca (R.S. Russell).

0168-1702
http://dx.doi.org/10.1016/j.virusres.2013.06.008

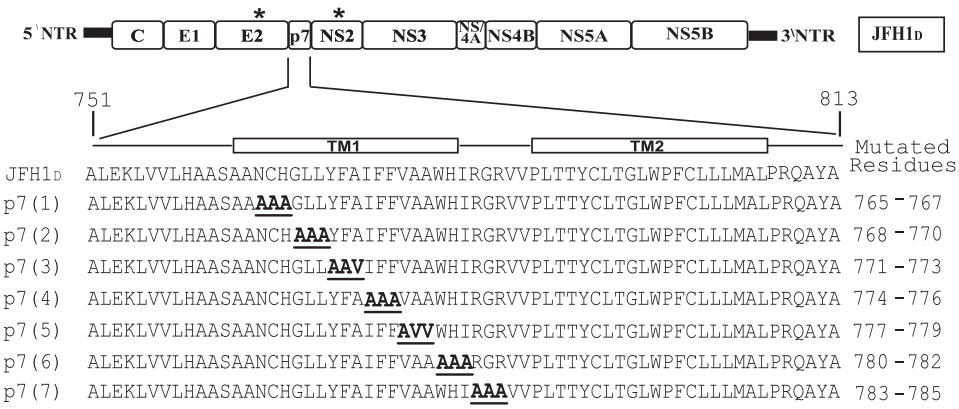

Fig. 1. Construction of p7 mutants. Seven alanine triplet mutants were constructed in the background of $JFH1_D$, which exhibits enhanced infectious virus production compared to JFH-1 due to the presence of adaptive mutations in E2 (N417S) and NS2 (Q1012R), (indicated by *). The p7 TM1, TM2 and the cytoplasmic loop with the amino acid compositions are shown, with mutated residues in bold and underlined, and affected polyprotein aa numbers on the right. Valine was introduced at positions where the original amino acid was alanine.

involved in viral RNA replication, but are believed to be involved in viral assembly and/or release (Jones et al., 2007; Steinmann et al., 2007; Jirasko et al., 2008, 2010; Popescu et al., 2011a,b; Stapleford and Lindenbach, 2011; de la Fuente et al., 2013).

The viral protein p7 was first identified by expression of a series of C-terminally truncated HCV polyproteins fused to a human *c-myc* epitope tag, which mapped it between E2 and NS2 (Lin et al., 1994). HCV p7 is a 63aa protein that localizes to the ER and contains two transmembrane domains (TM1 and TM2) connected by a short cytoplasmic loop with both the amino- and carboxy-termini oriented toward the lumen (Carrere-Kremer et al., 2002). The only functional study of p7 *in vivo* indicated that p7 is essential for successful intrahepatic infection in the chimpanzee model and illustrated its critical role in the viral life cycle (Sakai et al., 2003). Furthermore, p7 was shown to homo-oligomerize and possess ion channel activity in artificial lipid bilayers *in vitro* (Griffin et al., 2003; Pavlovic et al., 2003; Griffin et al., 2004; Luik et al., 2009). This activity has led to the inclusion of p7 into a group of proteins called viroporins, such as M2 of influenza virus and Vpu of HIV-1, which are capable of modulating membrane permeability in order to assist in viral entry, assembly or release (Wang et al., 2011). The ion channel activity of p7 is sensitive to multiple ion channel inhibitors such as amantadine and rimantadine in a genotype-dependent manner (Griffin et al., 2008). However, only amantadine in combination with pegylated interferon and ribavirin has been studied in clinical trials, but showed limited efficacy with inconclusive antiviral activity (Castelain et al., 2007).

While it is known that p7 is important for the production of infectious virus, there is some debate as to the exact step at which p7 acts. For example, some studies employing full-length HCV chimeras have indicated that p7 acts at a late stage during viral assembly and release (Steinmann et al., 2007; Yi et al., 2007), whereas other work indicated that p7 functions at an early stage during virion morphogenesis (Jones et al., 2007). It has also been shown that p7 interacts with NS2 and that this interaction is required for efficient viral assembly and release (Jirasko et al., 2010; Boson et al., 2011; Ma et al., 2011; Popescu et al., 2011a,b; Vieyres et al., 2013). In addition, a comprehensive study that aimed to characterize the contribution of p7 to organelle pH regulation and virus production showed that during HCV infection, p7 could equilibrate intracellular vesicle pH and reduce the number of highly acidic vesicles more rapidly than ion channel defective p7 mutant sequences. This study also showed that H^+ conductance was sensitive to viroporin inhibitors (Wozniak et al., 2010). These results indicate that exposure to acidic pH renders HCV particles non-infectious. However, exactly how this pH-regulating function of p7 affects the virus itself remains an important question.

The aim of this study was to further elucidate the role of p7 in the HCV life cycle through the use of a highly adapted version of JFH-1 containing previously described adaptive mutations (Russell et al., 2008). We have performed an extensive mutagenesis analysis of p7 by creating multiple alanine triplet mutations spanning TM1 and the cytoplasmic loop. These mutant virus genomes were analyzed for their effects on infectious virus production in both multiple- and single-cycle virus production assays. Detailed functional characterization of the effects of these mutations at multiple stages of the HCV life cycle were then performed, including polyprotein processing, core/lipid droplet association, core protein oligomerization and virus release.

2. Materials and methods

2.1. Cell culture

Transfections and infections were performed in Huh-7.5 cells (generous gift from C.M. Rice, Rockefeller University/Apath Inc. LLC, USA; Blight et al., 2002) and S29 cells (subclone of Huh-7 cells representing a single-cycle virus production assay (Russell et al., 2008), generous gift from S. Emerson, NIH, USA). Both cell lines were cultured in Dulbecco's Modified eagle's medium (DMEM, Invitrogen) supplemented with 10% fetal calf serum and 1% penicillin/streptomycin, referred to as complete medium. All cells were grown at 37 °C in 5% CO_2.

2.2. Cloning and plasmid construction

Plasmids were constructed in the backbone of $JFH1_D$ (adapted genotype 2a genome; Fig. 1). PCR mutagenesis was employed to introduce the desired mutations (Fig. 1) with primers that included the *Bsi*WI and *Not*I restriction sites within the $JFH1_D$ backbone. The $JFH1_D$ plasmid and PCR products were digested with *Bsi*W1 and *Not*1 (New England Biolabs) and fragments gel-purified then ligated using the Rapid DNA Ligation Kit (Roche). The ΔGDD negative control was created using the QuikChange II XL Site-Directed Mutagenesis Kit (Agilent Technologies), using specific primers that omitted the GDD motif of NS5B. The same strategy was also employed to create the $JFH1_{A4S}$ backbone using a primer encoding the E1 A4 epitope in the backbone of $JFH1_S$, which includes only the NS2 adaptive mutation. The p7 mutations were then recreated by substituting the *Bsi*WI and *Ale*I digested fragment from the original p7 mutant plasmids into $JFH1_{A4S}$. All plasmid sequences were

verified by enzymatic digestion and double-stranded DNA sequencing. All primer sequences and detailed information regarding the cloning procedures are available upon request. Note that the adaptive mutations present within each construct ($JFH1_D$, $JFH1_S$ and $JFH1_{A4S}$) are described in Section 3 the first time that they are mentioned.

2.3. In vitro transcription and RNA transfection

Mutant and control plasmids were linearized by *Xba*I digestion for 2 h at 37 °C and 1 μg of each linearized plasmid was used for *in vitro* RNA transcription using the T7 Megascript kit (Ambion). RNA integrity was verified by gel electrophoresis. RNA transcripts were transfected using DMRIE-C reagent (Invitrogen) into 1×10^6 Huh-7.5 or S29 cells plated in 10 cm cell culture dishes 24 h prior to transfection.

2.4. Antibodies

The following antibodies were used in this study: Mouse anti-core monoclonal antibody (mAb) (B2; Anogen) was used for both indirect immunoflouresence at a dilution of 1:200 and Western blotting analysis at a dilution of 1:1000; Mouse anti-NS3 mAb at a dilution of 1:5000 (C65371M; Meridian Life Science); Mouse mAb A4 (anti-E1; a kind gift from Harry Greenberg, Stanford, USA; Dubuisson et al., 1994); Mouse anti-NS2 (6H6, a kind gift from Charles M. Rice, Rockefeller University, USA; Dentzer et al., 2009) both used for Western blot analysis at dilutions of 1:2000; Mouse anti-E2 (AP33; generous gift from Genentech, USA/Arvind Patel, MRC-University of Glasgow, UK; Clayton et al., 2002) used at a dilution of 1:1000; Mouse anti-GAPDH mAb at a dilution of 1:10,000 (Abcam); sheep anti-NS5A antiserum (a kind gift from Mark Harris, University of Leeds, UK) used for Western blot analysis at dilutions of 1:10,000. HCV core in gradient analyses was detected using mouse anti-core mAb (MA1-080; Pierce Research) at a dilution 1:1000, and mouse anti-ADRP (Progen Biotechnik) was used at a dilution of 1:1000. Alexa Flour® 488 anti-mouse secondary antibody (Invitrogen) was used for indirect immunoflourescence at a dilution 1:1000. Goat anti-mouse and donkey anti-sheep HRP-labeled secondary antibodies (Santa Cruz Biotechnology) were used for Western blot analysis at a dilution of 1:1000.

2.5. Indirect immunofluorescence

Cells were grown on 8-well chamber slides (Thermo Scientific), fixed in 100% acetone for 2 min, washed with phosphate buffer saline (PBS) and incubated with primary antibody for 20 min. Then, slides were washed 3 times with PBS and incubated with the secondary antibody for an additional 20 min and washed 3 times with PBS. Slides were then mounted with Vectashield Hard Set mounting medium containing DAPI (Vector Laboratories).

2.6. Virus titration

Virus titers were determined by endpoint dilution assay for focus-forming units (ffu) as described previously (Zhong et al., 2005). Briefly, 8-well chamber slides were seeded with 4×10^5 Huh-7.5 cells per well 24 h prior to infection. At 72 h post-transfection, cell supernatants were clarified through Millex-HV 45 μm filters (Millipore) before being serially diluted 10-fold with complete DMEM. 100 μl of each dilution was inoculated for 4 h before being removed and replaced with complete DMEM. At 72 h post-infection cells were fixed and visualized by indirect immunofluorescence for core protein. Virus titers were expressed as the number of ffu per ml of supernatant, where a focus was defined by a cluster of 3 or more infected cells.

2.7. Titration of intracellular infectious virus

At 72 h post-transfection, cells were trypsinized, pelleted by centrifugation at $400 \times g$ and re-suspended in 1 ml of complete DMEM. The re-suspended cells were then lysed by 4 cycles of freeze/thaw (3 min freeze/3 min thaw) in a dry ice/methanol bath and pelleted by centrifugation at $1500 \times g$. Virus titers were determined as described above.

2.8. SDS-PAGE and Western blotting analysis

At indicated time-points post-transfection, cells were trypsinized, pelleted by centrifugation at $400 \times g$ and re-suspended in 300 μl of passive lysis buffer (Promega). Cellular debris was pelleted by centrifugation after 30 min incubation on ice. A fraction of the cell lysates was then loaded in a 1:1 ratio with 2× loading dye for SDS-PAGE. To visualize extracellular core protein, at 72 h post-transfection 12 ml of transfection supernatant (pooled from 2 × 10 cm dishes) was passed through a 0.45 μm filter and subjected to ultracentrifugation at $80{,}000 \times g$ for 4 h at 4 °C using a Sorvall TH-614 rotor. Pellets were re-suspended in 20 μl of 2× loading dye and the full amount was subjected to SDS-PAGE and Western blotting.

2.9. Confocal microscopy

At 72 h post-transfection, cells were seeded onto 8-well chamber slides and 48 h later washed with PBS and fixed with 4% Paraformaldehyde for 20 min, then washed and permeabilized with 0.1% Triton X-100 for 15 min. Following this, cells were washed and incubated with anti-core Ab at a 1:200 dilution in 5% BSA/PBS. Next, cells were washed 3 times and incubated with anti-mouse Alexa Fluor® 488. To visualize lipid droplets the HCS LipidTOX Deep Red neutral lipid stain (Invitrogen) was added to Vectashield Hard Set mounting medium containing DAPI (Vector Laboratories) at a 1:200 dilution then added to the slides and examined by laser scanning confocal microscopy.

2.10. Iodixanol density gradient fractionation

Two 10 cm plates per construct were transfected as described above and cells were trypsinized 72 h post-transfection, pelleted by centrifugation and re-suspended in 0.5 ml of lysis buffer (50 mM Tris (pH = 7.5), 140 mM NaCl, 5 mM EDTA and 0.5% Triton-X100) and incubated for 30 min on ice then cleared by centrifugation. The clarified 0.5 ml were loaded over 4.5 ml of pre-formed 10–50% iodixanol gradients (prepared using OptiPrep Density Gradient Medium (Sigma) and Hank's Balanced Salt solution (Invtrogen)). Samples were then ultracentrifuged at $100{,}000 \times g$ for 16 h at 4 °C using a Beckman SW55Ti rotor. Next, ten fractions (0.5 ml/fraction) for each construct were collected from the top of each tube. 50 μl from each fraction was retained before the protein precipitation process for measurement of density of each fraction using a refractometer (Fisher Scientific). Detailed protocols are available upon request. Proteins were extracted from the remainder of each fraction by methanol precipitation at −20 °C for 40 min, and then pelleted by centrifugation. The resultant pellets were re-suspended in 50 μl of 2× loading buffer, boiled and then probed for core protein by Western blot analysis.

2.11. Bafilomycin A1 and NH_4Cl treatments

4 pM Bafilomycin A1 (dissolved in DMSO) and 12 mM NH_4Cl were prepared and used to treat Huh-7.5 or S29 cells that had received mutant or control RNA 48 h previously. These concentrations were chosen after testing a range of 1–50 pM (Bafilomycin A1) and 6–50 mM (NH_4Cl). Supernatants from harvested cells were used for titer determination or Western blot as outlined previously.

3. Results

3.1. Mutations within TM1 and the cytoplasmic loop reduce infectious virus production

Previous reports have identified adaptive and compensatory mutations within p7 that enhanced virus production (Zhong et al., 2006; Delgrange et al., 2007; Kaul et al., 2007; Yi et al., 2007; Di Giorgio et al., 2008; Russell et al., 2008). The cytoplasmic loop region contains highly conserved basic residues, K33 and R35, known to impact infectivity in chimpanzees, as well as *in vitro* ion channel activity and virus production in cell culture (Sakai et al., 2003; Griffin et al., 2004; Jones et al., 2007; Steinmann et al., 2007). Based on these findings we hypothesized that a comprehensive mutational analysis of TM1 and the cytoplasmic loop might provide additional insight into the function of this protein. Accordingly, seven alanine triplet mutations (termed p7(1)–p7(7)) were generated to cover the TM1 and cytoplasmic loop of p7 (Fig. 1). These mutations were constructed in the background of a full-length, cell culture-adapted strain of HCV JFH-1 termed $JFH1_D$, which contains two adaptive mutations in E2 (N417S) and NS2 (Q1012R) that function cooperatively to increase infectious virus production (Russell et al., 2008).

To test the effects of the generated mutations on infectious virus production, we used a single-cycle virus production assay. Here, the mutant RNA genomes were transfected into S29 cells, which express very low levels of CD81, the major receptor for HCV entry (Russell et al., 2008). These cells permit RNA replication and virus particle production, yet do not support virus entry, allowing a comparison between mutants and their ability to generate infectious progeny without the confounding effects associated with multiple infectious cycles. Core, NS3 and NS5A Western blot analyses performed on transfected S29 cell lysates at 72 h post-transfection showed similar band intensities among the mutants when compared with $JFH1_D$, indicating that transfection efficiencies were comparable and protein expression/processing was not affected by the mutations generated in p7 (Fig. 2A). These comparable protein levels also exclude possible effects on RNA replication or genome instability that may have been caused by the generated mutations. The negative control (ΔGDD) contains a deletion within the active site of the HCV NS5B polymerase, and therefore produced no core, NS3 or NS5A.

At 72 h post-transfection, S29 cells were trypsinized and re-plated in 8-well chamber slides. Two days later indirect immunofluorescence analysis confirmed that all mutant genomes and the $JFH1_D$ control possessed relatively similar HCV core staining patterns, with approximately 25% of cells being positive for core (Fig. 2B). Cells transfected with ΔGDD displayed no core-positive cells.

Next, to quantify the effects of the generated mutations on virus production, we measured the levels of infectious virus present in the supernatants of transfected cells (Fig. 2C). Mutation p7(1), (located at the amino-terminal end of TM1) p7(4), (near the carboxy-terminal end), as well as mutations p7(6) and p7(7) (within the cytoplasmic loop) reduced infectious virus production to levels lower than the detection limit of the assay. In contrast, p7(2) and p7(3), located in the central region of TM1, decreased virus production by ~2 logs. The mutation near the carboxy-terminal end of TM1 (p7(5)) showed little effect on virus production, which was likely due to the conservative amino acid changes comprising this mutation (VAA-AVV). Taken together, these data indicated that TM1 and the cytoplasmic loop of p7 are important for infectious virus production, and that the amino acids located within the central region of TM1 are seemingly less critical for p7 function.

To verify these findings, we repeated the above experiments in Huh-7.5 cells and found that the levels of core, NS3 and NS5A proteins on Western blots were apparently different among the mutant viruses (Supporting Fig. 1A). Core immunofluorescence staining patterns were also different from that observed in S29 cells (Supporting Fig. 1B), demonstrating that mutations p7(1), p7(4), p7(6) and p7(7) substantially affected virus spread. Mutant virus p7(5) exhibited similar core staining to that of $JFH1_D$ with >90% of the cells positive for core. The ΔGDD control displayed no core signal. Virus production at 72 h post-transfection of Huh-7.5 (Supporting Fig. 1C) was higher than that from S29 cells (Fig. 2C), but overall patterns between mutants were similar (minor differences between cell lines for p7(1) and p7(6) were disregarded since they fell under the assay cut-off). The observed differences on protein levels, core staining patterns and virus titers correlated with the effects of virus spread and are therefore due to the amplification and accumulation of virus that occurs in the permissive Huh-7.5 cells, which is in agreement with previous findings (Jones et al., 2011). These results indicated that the generated mutant genomes are indeed defective in infectious virus production.

Supplementary data associated with this article can be found, in the online version, at http://dx.doi.org/10.1016/j.virusres.2013.06.008

3.2. Analysis of intracellular and extracellular species of virus particles

The reduction of extracellular infectious virus exhibited by some of the p7 mutants could result from two possibilities: (i) p7 mutants exhibit wild-type levels of released virus particles, but these have reduced infectivity, or (ii) an overall reduction in the production of particles. To determine which of these possibilities occurred in the case of our mutants, supernatants from Huh-7.5 cells transfected with the mutants and controls were collected at 72 h post-transfection, clarified, layered over a 20% sucrose cushion and subjected to ultracentrifugation. Huh-7.5 cells were used in this case to maximize yields of virus. Western blot analysis was then performed on the pelleted material (Fig. 3A). Core protein was detectable only for genomes that produced significant levels of infectious particles ($JFH1_D$ and p7(5)), demonstrating that the mutations introduced into p7 decreased the production of core-containing particles, as opposed to reducing the infectivity of secreted virions.

From the results outlined above, we next investigated whether the p7 mutants that produced little or no extracellular infectivity were also compromised for intracellular infectivity. Accordingly, S29 cells transfected with p7 mutants and controls were subjected to multiple freeze/thaw cycles to obtain intracellular infectious virus at 72 h post-transfection. In parallel, filtered supernatants were collected and viruses from both sources were used to inoculate naïve Huh-7.5 cells to measure infectious titers (Fig. 3B). All mutants with lowered extracellular titers also displayed similar reductions in the levels of intracellular infectious virus. Taken together, these results demonstrate that the mutations made within p7 resulted in an absence of core-containing HCV particles

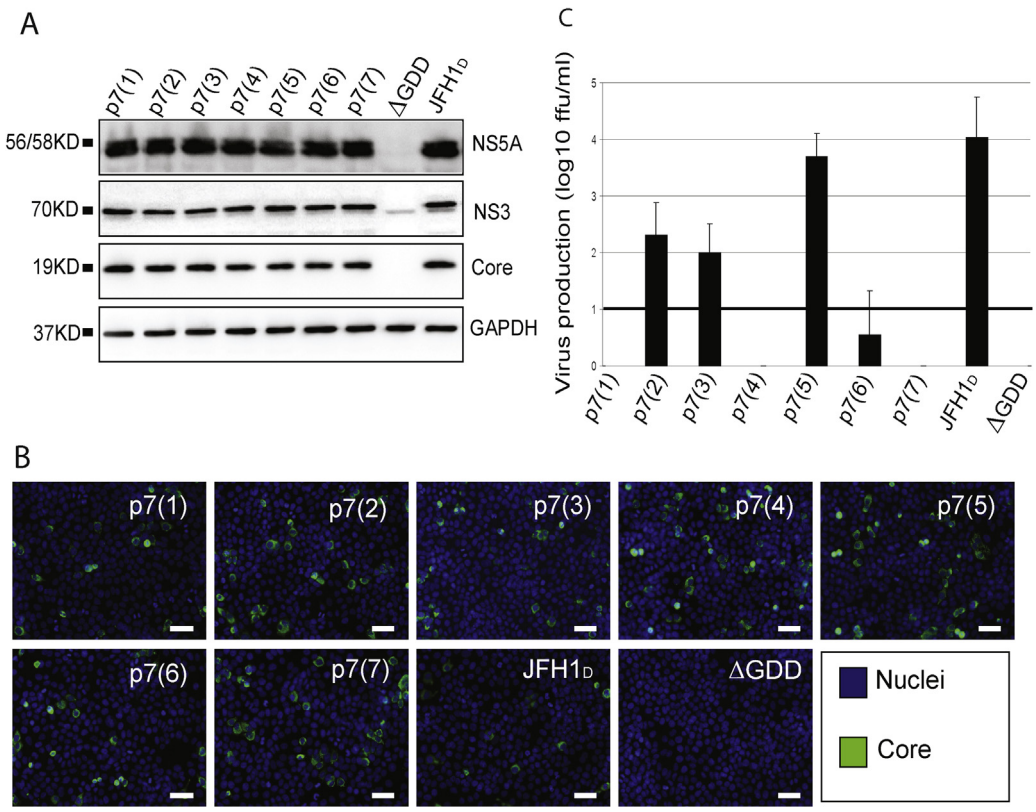

Fig. 2. Single-cycle virus production assay analysis of p7 mutant viruses. (A) S29 cells transfected with the p7 mutants or controls ($JFH1_D$ and ΔGDD) were lysed and probed with antibodies recognizing core, NS3, NS5A and GAPDH by Western blot analysis. (B) S29 cells were transfected with equivalent amounts of transcribed RNA representing p7 mutants and controls ($JFH1_D$ and ΔGDD). At 72 h post-transfection, cells were seeded onto 8-well chamber slides and two days later washed, fixed and stained for core (green) and DAPI (blue). Scale bars represent 50 μm. (C) Culture supernatants were filtered and serially diluted to infect naïve Huh-7.5 cells. At three days post-infection virus titers were determined by limiting dilution focus-forming assay. Focus-forming assays were performed in triplicate and error bars represent standard error of the mean. The bold line represents the cut off of the assay, which was 10 ffu/ml. Results are representative of three independent transfection/infection experiments. (For interpretation of the references to color in this figure legend, the reader is referred to the web version of this article.)

outside the cell, most likely resulting from their compromised ability to generate infectious particles in the intracellular environment.

3.3. Mutations in p7 TM1 and the cytoplasmic loop do not affect core sedimentation profiles

The above data indicated that the selected p7 mutations within TM1 and the cytoplasmic loop are unable to produce intracellular infectious virions. However, it was unclear whether these mutants were assembling intracellular particles that were non-infectious, or were incapable of building the nucleocapsid structure. Typically, density gradient fractionation of transfected cell lysates has revealed that intracellular HCV core exists at various densities, presumably representing sequential stages of capsid assembly. These species are thought to include monomeric core associated with LD, and oligomerized core representing both newly-forming nucleocapsids and virions associated with triglycerides and β-lipoprotein (VLDL and LDL) complexes (Andre et al., 2002; Gastaminza et al., 2006; Alsaleh et al., 2010; Jones et al., 2011). Therefore, we sought to determine whether any of our p7 mutants displayed altered patterns of core distribution following centrifugation through density gradients.

To do this, two mutations within TM1 (p7(2) and p7(4)) and one mutation within the cytoplasmic loop (p7(7)) were selected for gradient analysis because they spanned the TM1 and cytoplasmic loop region of p7. Also, these mutants displayed a spectrum of effects on virus production; (p7(2)) showed a moderate reduction, whereas p7(4) and p7(7) produced no detectable infectious virus. These mutant RNA genomes were transfected into Huh-7.5 cells, and 72 h later, intracellular lysates were harvested using TNE buffer containing 0.5% Triton X-100. This mild detergent was chosen to preserve core-core oligomers within the lysate while disrupting core-membrane complexes that may otherwise be sufficiently dense to traverse into the gradient and be misinterpreted as multi-ordered structures. Lysates were then loaded over 10–50% iodixanol gradients and subjected to ultracentrifugation. Ten gradient fractions were collected from top (fraction 1) to bottom (fraction 10) and analyzed by Western blot for core (Fig. 4). In all constructs tested, varying core protein levels were observed in fractions 1–3, likely representing monomeric core species (densities ranging from 1.019 to 1.090 g/cm^3) (Fig. 4). The strongest core bands, which we propose represent naked viral nucleocapsids, typically appeared in fractions 6 and 7 with a density range of 1.145–1.169 g/cm^3. It is unlikely that these core structures were enveloped/complexed with membranes, since no infectivity was associated with these (or any) fractions. While slight variations were regularly observed in these assays, we did not observe any consistently noticeable differences between $JFH1_D$ and any of the p7 mutants tested with respect to core patterns on Western blots, except that $JFH1_D$ showed higher core band intensities in the blots due to its ability to spread and produce more infectious virus. However, using a lysis buffer containing a detergent capable of breaking core-core interactions (TNE + 0.5% SDS) resulted in a loss of core from fractions 6 and 7, with most of the protein now being found in the top fractions of the gradient (Fig. 4).

It should be noted that a comparison of lysis methods (freeze-thaw versuss TNE + 0.5% TX-100) on cells harboring $JFH1_D$ revealed differences in core banding patterns, indicating that these distinct

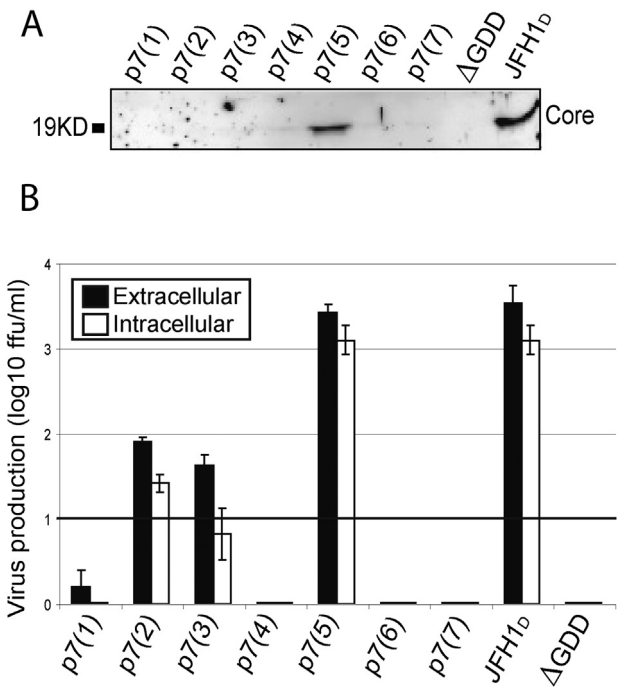

Fig. 3. Extracellualr particls production and comparison of intracellular *vs.* extracellular infectious virus. (A) Huh-7.5 cells were transfected with equivalent amounts of transcribed RNA representing p7 mutants and controls ($JFH1_D$ and ΔGDD) for 72 h. 12 ml of supernatants (pooled from two 10 cm dishes) representing p7 mutants and controls were loaded over 2 ml of 20% sucrose, ultracentrifuged and the pellet probed by Western blot for core protein. Results are representative of two independent transfection/infection experiments. (B) S29 cells were transfected as above and 72 h post-transfection extracellular (solid bars) and intracellular (open bars) infectious virus production were measured by focus-forming assay in triplicate, and means plus standard errors are plotted. Results are representative of two independent transfection/infection experiments.

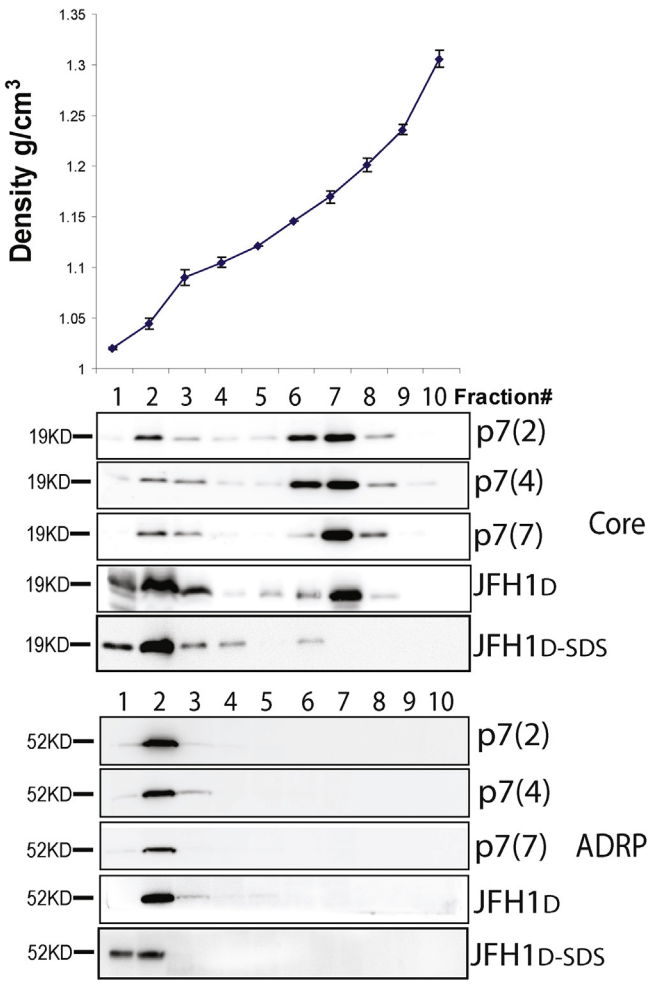

Fig. 4. Iodixanol gradient analysis of p7 mutant viruses. Huh-7.5 cells were transfected with RNA representing selected p7 mutant viruses including TM1 mutants p7(2) and p7(4) as well as the cytoplasmic loop mutant p7(7), and $JFH1_D$ was used as a control. At 72 h post-transfection intracellular lysates were harvested, loaded over preformed 10–50% iodixanol gradients and subjected to ultracentrifugation. Ten fractions from each tube were collected from top (fraction 1) to bottom (fraction 10) Density measurements (g/cm^3) on each fraction were measured using a refractometer (top panel), and Western blot analyses for core and ADRP were performed (middle and bottom panels). Results are representative of three independent transfection/infection experiments.

lysis methods influence the migration of liberated core through iodixanol gradients (Supporting Fig. 2). However, we also observed no differences between p7 mutants and $JFH1_D$ when lysates were prepared by freeze-thaw (data not shown). Similarly, spinning harvested intracellular particles through a sucrose cushion prior to their ultracentrifugation through an iodixanol gradient made little difference (with the exception of filtering out core in fractions 1–3) to those results obtained without a cushion (Supporting Fig. 2). Of further note is that RNA could not be measured for core-containing gradient fractions, since gradients run on a negative control (ΔGDD) also gave a peak of RNA in these fractions (data not shown). This final result suggests that gradient-derived RNA patterns obtained from intracellular lysates are complicated by the existence of input RNA delivered during the transfection process. Overall, the data obtained from density gradient experiments suggest that the p7 mutants tested here were competent for nucleocapsid assembly.

Supplementary data associated with this article can be found, in the online version, at http://dx.doi.org/10.1016/j.virusres.2013.06.008

3.4. p7 TM1 and the cytoplasmic loop do not affect core targeting to lipid droplets

We next wished to determine whether p7 might influence the recruitment of core protein to lipid droplets (LDs), the proposed platform for virion formation (Miyanari et al., 2007). Accordingly, Huh-7.5 cells were transfected with the mutant genomes and stained for core protein and LDs 72 h later. Huh-7.5 cells were used in this experiment in order to maximize the number of core-positive cells available for observation. As shown in (Fig. 5), no differences in core/LD association were observed between the $JFH1_D$ control and any of the p7 mutants tested. These data conclusively demonstrate that neither p7 TM1 nor the cytoplasmic loop affect the targeting of core protein to LDs, and that any reductions observed in infectious virus production did not result from failed loading of core onto the surface of LDs.

3.5. Mutation of the p7 cytoplasmic loop results in a time-dependent reduction of E2 levels

It has previously been shown that p7 can regulate pH in intracellular compartments (Wozniak et al., 2010), presumably to protect the virus from acid-induced degradation during viral egress. However, p7 may have an additional, separate function that involves an interaction with NS2, and this interaction may be important for localization of p7 with other viral proteins, including core and E2, at the site of assembly (Jirasko et al., 2010; Boson et al., 2011; Ma et al., 2011; Popescu et al., 2011a,b; Vieyres et al., 2013). Therefore, it became essential to test some of our p7 mutants for an

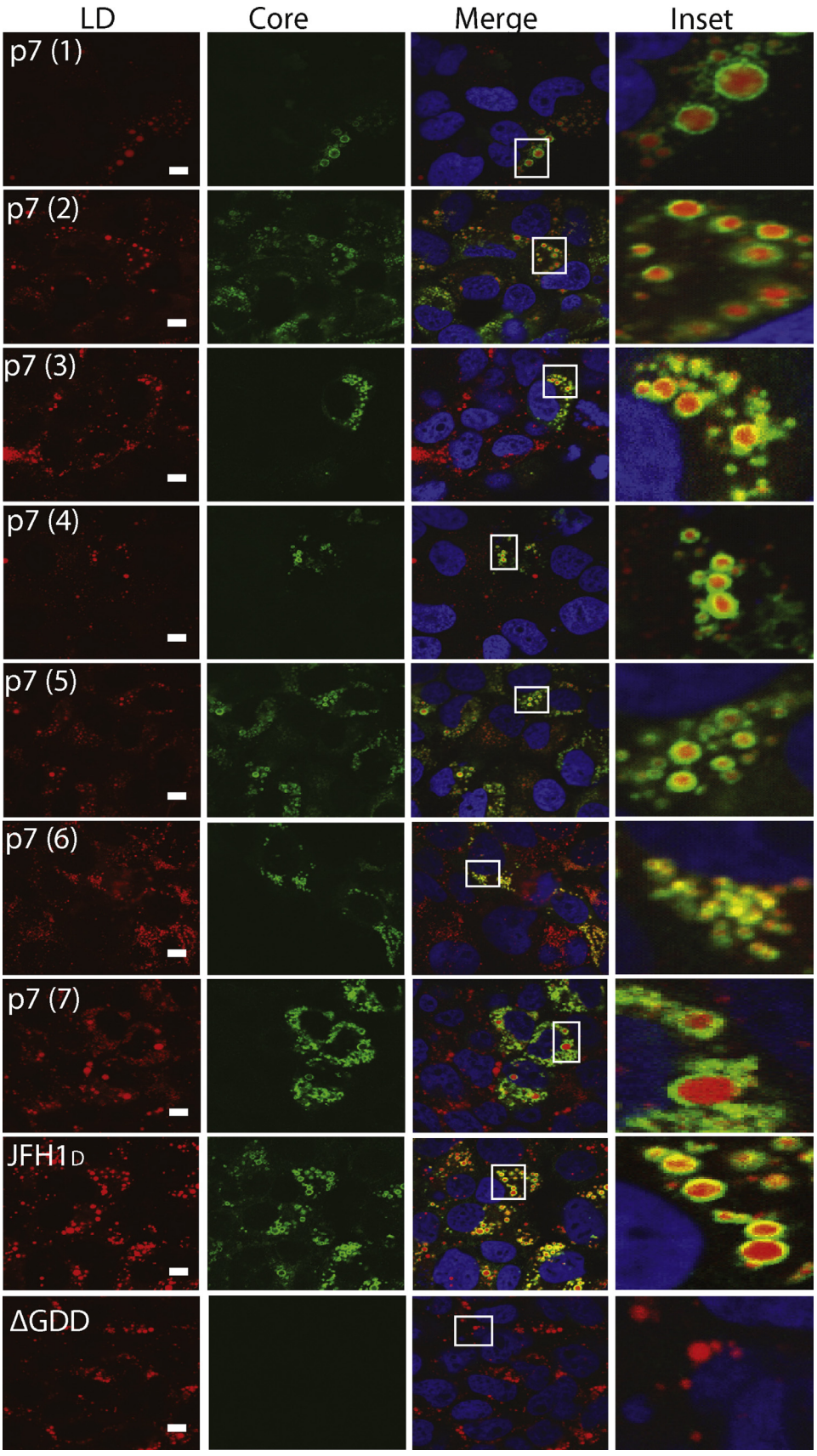

Fig. 5. Analysis of core/lipid droplet association. Huh-7.5 cells were transfected with equivalent amounts of transcribed RNA representing p7 mutants and controls ($JFH1_D$ and ΔGDD). At 72 h post-transfection, cells were seeded onto 8-well chamber slides and two days later washed and stained as described above. Cells were visualized by confocal microscopy under oil immersion. Scale bars represent 10 μm. Enlarged areas from the merged image are shown on the right. Blue represents DAPI-stained nuclei, green fluorescence represents HCV core protein and red represents lipid droplet staining. Results are representative of three independent experiments. (For interpretation of the references to color in this figure legend, the reader is referred to the web version of this article.)

effect on viral glycoproteins E1 and E2. To do this, we first generated two new constructs–JFH1$_S$ and JFH1$_{A4S}$. JFH1$_S$ is the same as JFH1$_D$, except that it lacks the N417S adaptive mutation in E2. This construct had to be used for E2 analyses because N417S is located within the epitope recognized by most antibodies that bind JFH-1 E2, thereby preventing detection. In turn, JFH1$_S$ was further modified by substituting a short sequence of E1 for the analogous sequence from HCV strain H77, to produce JFH1$_{A4S}$. This strategy, reported elsewhere, renders E1 detectable by the E1 antibody A4 (Stapleford and Lindenbach, 2011). The modifications required to produce both these new constructs did reduce virus production by approximately 15-fold (JFH1$_S$) and 70-fold (JFH1$_{A4S}$) compared to JFH1$_D$ (Supporting Fig. 3). However, virus production remained sufficient for analysis.

Supplementary data associated with this article can be found, in the online version, at http://dx.doi.org/10.1016/j.virusres.2013.06.008

To examine effects on both E1 and E2, we first introduced selected p7 mutations (1, 3, 4, 6 and 7) into the background of JFH1$_{A4S}$. Upon transfection of Huh-7.5 cells with these p7 mutants, Western blot analysis indicated that all mutants displayed insignificant variations in core, NS2 and E1 protein levels (Fig. 6A). However, this was not the case for p7(7) (cytoplasmic loop mutant containing substitutions in the two conserved basic residues), where a substantial reduction in E2 was apparent. These results were confirmed in S29 cells (Fig. 6A). To analyze the reduction in E2 more quantitatively, the Western blot band intensities for E2 were measured by densitometry relative to that of core expressed from each mutant. Additionally, NS2 levels were measured in this manner (Fig. 6B). This analysis conclusively demonstrated that E2 levels expressed from p7(7) were significantly lower compared to JFH1$_{A4S}$ and the other p7 mutants, whereas NS2 levels remained unchanged (Fig. 6A and B). These results suggest that modification of the dibasic residues within the p7 cytoplasmic loop leads to a reduction of E2 glycoprotein levels.

Previous reports have demonstrated that alteration of the p7 cytoplasmic loop can result in the detection of E2-p7-NS2 precursors by Western blot (Steinmann et al., 2007). While we did not observe this effect in Fig. 6A, E2 and NS2 blots were repeated using SDS-based Laemmli buffer in addition to our usual CHAPS-based buffer (Supporting Fig. 4). Here, we also saw no evidence for precursors on either the E2 or NS2 blots. Therefore, we presume that the observed phenotype for p7(7) resulted from direct effects on the protein itself rather than a processing defect. To further investigate the observed reduction of E2 in the p7(7) mutant, we carried out a time course analysis of E2 levels at 24, 48, and 72 h post-transfection in S29 cells. Since S29 cells are non-permissive for entry, they represent a relatively synchronized state of viral protein production upon transfection, which is ideally suited for this experiment. Here, the JFH1$_S$ strain of virus was used since it produces higher viral titers than JFH1$_{A4S}$ and detection of E1 was not required for this experiment. p7(1) was also included as an additional control since, like p7(7), it produces no infectious virus, yet generates near wild-type levels of E2. Lysates were prepared from each time-point and E2, core, and GAPDH levels were probed by Western blot (Fig. 6C). It was observed that at 24 h post-transfection the mutants and controls produced barely detectable levels of both E2 and core. By contrast, at the 48 h time-point, only p7(1) and the JFH1S$_{A4S}$ control displayed comparable levels of core and E2, with a slightly reduced amount of E2 in the case of p7(7). However, E2 levels expressed from p7(7) were noticeably reduced by 72 h compared to what they were at 48 h, as well as being diminished compared to the other constructs tested.

Supplementary material related to this article found, in the online version, at http://dx.doi.org/10.1016/j.virusres.2013.06.008

Finally, we attempted to rescue both infectious virus production and E2 levels from p7(7) by treating transfected cells with (i) Bafilomycin A1, to inhibit vesicular acidification as performed by others (Wozniak et al., 2010) and (ii) NH_4Cl, a lysosomal inhibitor (Supporting Fig. 5). However, we observed no restoration of virus production or E2 to levels seen with JFH1$_S$. Taken together, these results indicated that the mutations present in p7(7) appear to result in lower levels of E2, which cannot be restored through the inhibition of lysosome or vesicular acidification.

Supplementary material related to this article found, in the online version, at http://dx.doi.org/10.1016/j.virusres.2013.06.008

4. Discussion

The functionality of the p7 protein is one of the more poorly understood aspects of the HCV life cycle. p7 is important for both successful HCV infection in chimpanzees as well as virus production in cell culture, yet is seemingly dispensable for virus entry and RNA replication (Sakai et al., 2003; Jones et al., 2007; Steinmann et al., 2007; Brohm et al., 2009; Meshkat et al., 2009; Vieyres et al., 2013). Multiple studies indicate that p7 forms ion channels in artificial membranes, leading to its inclusion in the viroporin protein family (Griffin et al., 2003; Pavlovic et al., 2003; Premkumar et al., 2004). Recently, amino acids required for the ion channel activity of p7 were also shown to be important for pH modulation of intracellular vesicles in cell culture, and this activity was important for maintaining infectious virus production (Wozniak et al., 2010). In this study, we performed an extensive mutational analysis to determine at which stage of the viral life cycle p7 acts. Alanine triplet mutations spanning TM1 and the cytoplasmic loop were generated and tested for their ability to produce virus, and subsequently, other stages of the viral life cycle were probed. The data indicated that regions of both the cytoplasmic loop and TM1 of p7 are important for virus production. p7 was not involved in virus release as reductions in both intra- and extracellular infectious virus were observed. Furthermore, mutating these regions of p7 did not alter core localization to lipid droplets, and capsid assembly was seemingly unaffected. Most importantly, we observed that alanine substitution of the two basic residues within the cytoplasmic loop of p7 caused a reduction in the amount of E2 present in transfected cells.

The cytoplasmic loop of p7 links the two TM helices and harbors a conserved dibasic motif, R33 and R35, which appear to be important for the ion channel activity (Griffin et al., 2004). The importance of the cytoplasmic loop in virus production was shown previously in multiple studies employing the HCVcc system, and *in vivo* after intrahepatic injection of chimpanzees (Sakai et al., 2003; Jones et al., 2007; Steinmann et al., 2007). Most of these studies concentrated on the cytoplasmic loop, especially the R33 and R35 residues, since it was previously shown that these residues were important for p7 ion channel activity in artificial membrane assays (Griffin et al., 2004). In this study we performed a comprehensive, side-by-side comparison of viruses containing mutations covering all of TM1 and the loop. We observed that the p7(7) mutant, which included the dibasic residues discussed above, and mutation p7(6), which is situated at the junction of the cytoplasmic loop and the TM1 helix, both terminated virus production. Moreover, a previous study created a W30F mutation, within the region that was also mutated in our p7(6), and found it to be an important residue for p7 function and virus production (Steinmann et al., 2007). Therefore, we have confirmed the importance of the cytoplasmic loop structure in virus production.

The data herein also showed that residues within TM1 are important for virus production, with the greatest effects observed for mutations at both N- and C-terminal ends of TM1. This

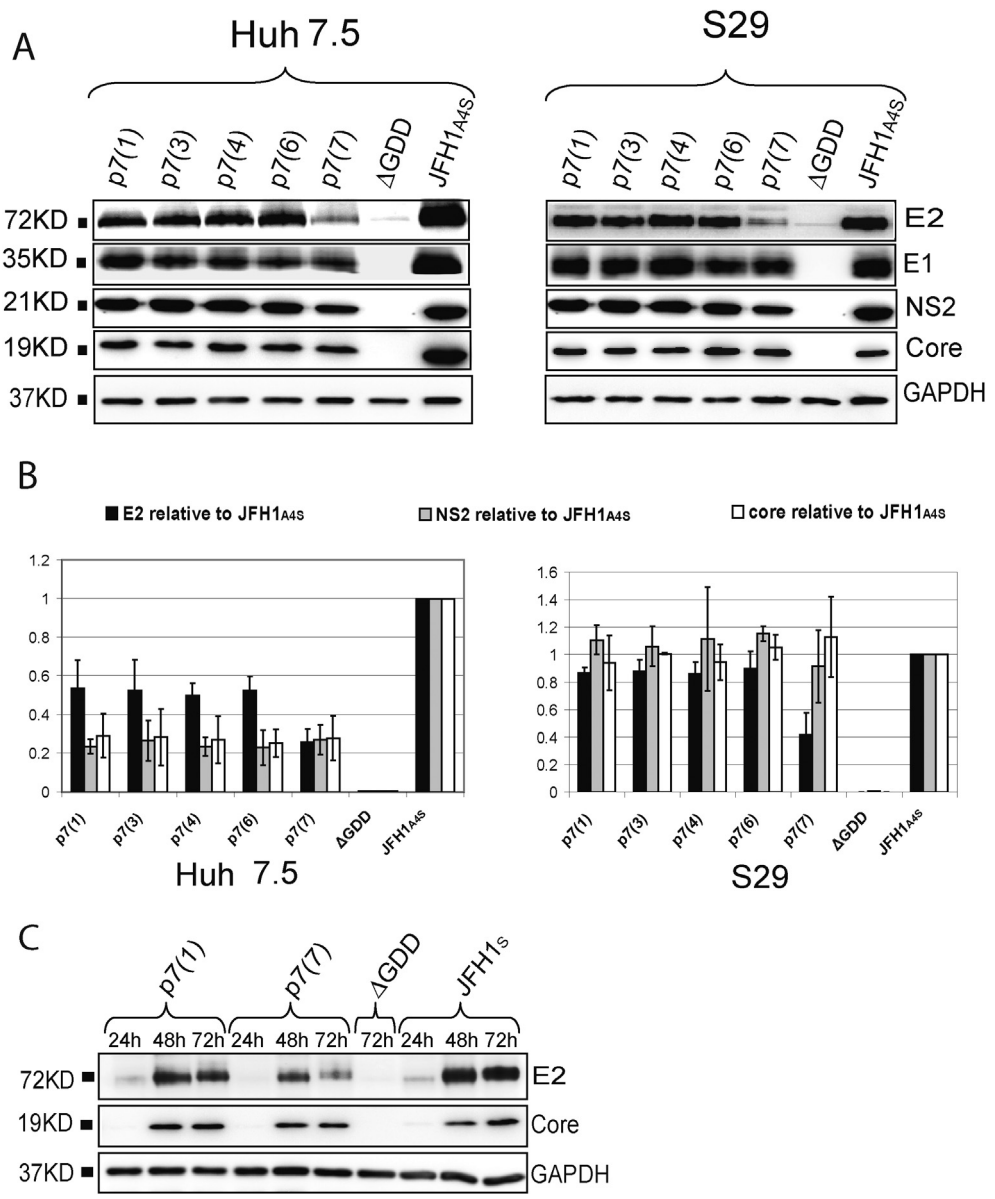

Fig. 6. Effects of p7 mutations on E2 levels. (A) Huh-7.5 and S29 cells were transfected with the indicated p7 mutants generated in the background of $JFH1_{A4S}$ along with appropriate controls ($JFH1_{A4S}$ and ΔGDD). At 72 h post-transfection, intracellular lysates were obtained and probed with antibodies against E1, E2, NS2, core, and GAPDH by Western blot. (B) Band intensity measurements for core and E2 where each mutant's band intensity was calculated relative to $JFH1_{A4S}$. (C) A time course of E2, core, and GAPDH expression by Western blot at 24, 48, and 72 h post-transfection of S29 cells for the mutants p7(1) and p7(7) generated in the background of $JFH1_S$. Results are representative of two independent experiments.

observation suggests that the positioning of the N- and C-termini of TM1 might be critical for anchoring the membrane-spanning region into the ER, and that mutation of this sequence may disrupt this positioning, thereby inhibiting virus production. Mutation of amino acids located near the N-terminal end of TM1 (p7(1)) caused a complete abrogation of virus production. This result is in agreement with a study showing that the H17 residue (H767 in the polyprotein of JFH-1) within TM1 is important for virus production and is part of a HXXXW-like motif found in the influenza virus M2 protein, which is the main functional element of the M2 channels (Meshkat et al., 2009). However, a separate study generated a single alanine substitution at residue N17 (N767 in the polyprotein of J6) in the context of the J6/JFH-1 chimeric virus and found an insignificant effect on virus production (Jones et al., 2007). These discrepancies might be explained by the chimeric nature of the viral backbone used in the later study, or may result from the triple alanine mutation studied here more drastically disrupting the M2-like motif. Interestingly, it has been previously reported that an adaptive mutation in this region (N15D; N765D in the JFH-1 polyprotein) enhanced virus production by 10-fold itself, further demonstrating the importance of these residues and suggesting that a putative interaction with other viral proteins is mediated by residues contained within the region mutated in p7(1) (Russell et al., 2008). Mutations p7(2) and p7(3) lie within the central region of TM1 and reduced virus production to approximately 50% of the levels observed with $JFH1_D$. The alanines substituted in this region replace uncharged hydrophobic amino acids (GLLYFA) and we propose therefore that these substitutions likely alter the optimal structure of this segment, but not sufficiently enough to terminate virion production. Others have also found this region to have a minimal effect on virus production (Jones et al., 2007). The p7(4) mutation completely abrogated virus production, indicating the

importance of one or more amino acids in this region. Interestingly, another study identified a compensatory mutation (F26L) at position F26 (also mutated in p7(4)) that rescued a mutation in the core protein (Murray et al., 2007), suggesting that p7 and core may work together through a direct interaction that has yet to be demonstrated. Thus, the targeted p7(4) residues might disrupt such an interaction. These results highlight that the integrity of both the N- and C-terminal regions of TM1 is important for the generation of infectious virus. It should also be noted that, as is usually the case for alanine-scanning mutagenic analyses, some of the constructed mutations were more conservative than others. For example, it was unsurprising that p7(5) (mutation from VAA to AAV) exhibited no reduction in virus production, most likely since the overall folding of p7 was largely unaltered due to the minor changes being introduced. This would not be the case for some of the other mutants, in which more drastic mutations were made, including p7(6) (mutation from WHI to AAA) and p7(7) (mutation from RGR to AAA). In the case of these latter mutants, we cannot exclude that virus production is abrogated due to p7 structural deformities resulting from the drastic amino acid changes.

During the early stages in virus assembly, core protein traffics to the surface of LDs and is proposed to serve as a platform for virion formation (Miyanari et al., 2007). Thus, we have tested our mutation at this stage and conclusively demonstrated that none of the p7 mutants tested affected core protein accumulation around lipid droplets. One recent study proposed that the core/LD association results from inefficient virus assembly, and that efficiently assembling viruses do not show significant levels of core/LD association (Boson et al., 2011). However, this was not the case in this study as the efficiently-assembling $JFH1_D$, as well as all virus production-defective mutants showed equivalent core/LD association.

The molecular details of HCV assembly are currently under intense investigation and are a matter of much debate. Following the recruitment of core to LDs, HCV capsid presumably begins to assemble through oligomerization of core, forming virus particles associated with one copy of the viral genome. This step presumably involves the production of multiple structures including oligomerized core representing both newly-forming nucleocapsids, and end-stage nucleocapsids associated with triglycerides and β-lipoprotein (VLDL and LDL). Evidence for this model is supported by the observed pattern of core distribution within density gradient analyses (Andre et al., 2002; Gastaminza et al., 2006; Alsaleh et al., 2010; Jones et al., 2011). In order to determine whether p7 plays a direct role in nucleocapsid assembly, we performed iodixanol gradient analyses on a select panel of p7 mutant viruses from cells that were lysed with a detergent-containing buffer. Based on the data shown in Fig. 5, we would conclude that p7 does not affect core assembly because we were able to detect dense species of core protein in fractions 6–8 of the gradient. However, while this manuscript was in revision an article was published by Gentzsch et al. (2013) that showed viruses lacking part of p7, or containing mutations in the loop, displayed an increased proportion of incompletely assembled capsids. At this point we cannot reconcile these different findings other than to note that different protocols were used in these two studies. For example, Gentzsch et al. (2013) performed sucrose-based rate zonal centrifugation on their mutants, whereas we used iodixanol equilibrium gradients. In subsequent studies we will be interested to determine whether we can identify nucleocapsid assembly defects in our mutants by rate zonal centrifugation.

Finally, Wozniak et al. (2010) found that p7 modulates intracellular proton conductance and increases lysosomal pH from 4.5 to 6.0 during HCV infection in cell culture. This report also demonstrated that the acidification inhibitor bafilomycin A1 and expression of influenza virus M2 protein restored virus production from a HCV genome mutated at the basic residues of the p7 cytoplasmic loop. Presumably, such a function would be important in protecting newly-formed virions from premature degradation at a late stage in virion production, specifically the envelope glycoproteins. We now show that a mutation within the loop that includes the same two basic residues also affected E2 protein expression and/or stability. It is logical to suspect that a lower pH could inactivate E2 by prematurely triggering conformational changes, but it is surprising that this would result in degradation of the glycoprotein, as we have observed. At this point we can only postulate that such a conformational change might either expose protease-sensitive regions of the protein or disrupt the stabilization provided by heterodimerization of E2 with E1. In any event, this result is in agreement with recently published work showing that a virus containing a defective p7 generated virions that were proteinase K-sensitive due to the lack of a viral membrane envelope. Bafilomycin A1 and MG132 did not restore virus production in our case, and this could be due to the possibility of the triple alanine substitution causing a complete abrogation of the ion channel activity or p7 topology. However, it is still unclear why this effect on E2 was only observed in the context of the cytoplasmic loop mutation (p7(7)). It is possible that p7 plays a dual role in the late viral assembly process, on one hand it could protect immature glycoproteins from degradation through an ion channel-like activity, but then could mediate proper targeting of viral glycoproteins to the assembly site. This potential dual role for p7 would explain the observation that other mutants, such as p7(1), p7(4) and p7(6) displayed similar reductions in virus production as did p7(7), but had no effect on E2 levels. This notion is supported by a study showing that pseudoreversion in p7 within TM1 of p7 (N15D) combined with a mutation at NS2 (G25R) restored virus infectivity and colocalization of NS2 around LDs along with E2 and NS3 (Jirasko et al., 2010), and these effects were not a consequence of p7 ion channel function (Tedbury et al., 2011). Also, Ma et al. showed that p7 deletion and mutations within the cytoplasmic loop affected the intracellular distribution of NS2 and E2 (Ma et al., 2011). Similarly, Staplford et al. found that NS2 interaction with other viral proteins was dependent on p7 coexpression (Stapleford and Lindenbach, 2011). Furthermore, Vieyres et al. recently constructed a functional HCV genome with a HA-tagged p7 and found that p7 interacted with NS2 and colocalized with E2 on the ER membrane (Vieyres et al., 2013). Therefore, it seems that p7 function may be two-fold: protection of virion-associated E2 from acid-induced degradation that is mediated by the ion channel activity subsequent to nucleocapsid formation and during envelopment. This function would have been disrupted by the p7(7) mutation studied herein, while in the second role, p7 is required for proper targeting of viral glycoproteins through a putative interaction between p7 TM1 and NS2.

5. Conclusion

We have demonstrated that p7 TM1 and the cytoplasmic loop are important for infectious virus production in cell culture. Our main finding is that disruption to the integrity of the conserved dibasic motif within the cytoplasmic loop of p7 results in diminished levels of E2 glycoprotein. Taken together with observations by other groups, we speculate that p7 acts at a point in the life cycle that is after nucleocapsid formation, but before virus release. In this way, we believe that p7 is important for viral envelopment, in that it protects E2 from premature degradation through an ion channel-like activity. Then, through a second function it is involved in interactions with other proteins in order to support late stage, post-nucleocapsid virus assembly. Further mutational studies covering the remainder of p7 and more extensive analysis of the E1 and E2 glycoproteins are required to better understand the mechanism of action of p7 and further emphasize its potential as a novel target for drug development.

Acknowledgements

This work was supported by research funding from the Canadian Institutes of Health Research (CIHR), Canada Foundation for Innovation, Research and Development Corporation of Newfoundland and Labrador (RDC), and the Faculty of Medicine, Memorial University of Newfoundland. AMA is supported by a CIHR/RPP/RDC fellowship for Allied Health Professionals. DMJ is supported by a Fellowship from the CIHR. RSR is a recipient of a CIHR New Investigator Award. The authors thank Robert Purcell and Sue Emerson (NIH, USA) for providing the JFH-AM1 adapted strain of JFH-1 and S29 cells, Takaji Wakita (National Institute of Infectious Diseases and Toray Industries, Inc., Japan) for provision of the JFH-1 infectious clone, and Charles Rice (Rockefeller University, USA and Apath, LLC, USA) for provision of Huh-7.5 cells. The authors would also like to thank Jackie Vanderluit for the use of her immunofluorescence microscope facility and Thomas Michalak for the use of his gradient mixer (both from Memorial University, Canada). Finally, we thank Harry Greenberg (Stanford, USA) for the A4 E1 antibody, Charles M. Rice (Rockefeller University, USA) for the anti-NS2 6H6 antibody, Genentech (USA)/Arvind Patel (MRC-University of Glasgow Center for Virus Research, UK) for the E2 AP33 antibody and Mark Harris (University of Leeds, UK) for provision of the anti-NS5A antiserum.

References

Alsaleh, K., Delavalle, P.Y., Pillez, A., Duverlie, G., Descamps, V., Rouille, Y., Dubuisson, J., Wychowski, C., 2010. Identification of basic amino acids at the N-terminal end of the core protein that are crucial for hepatitis C virus infectivity. Journal of Virology 84 (24), 12515–12528.

Andre, P., Komurian-Pradel, F., Deforges, S., Perret, M., Berland, J.L., Sodoyer, M., Pol, S., Brechot, C., Paranhos-Baccala, G., Lotteau, V., 2002. Characterization of low- and very-low-density hepatitis C virus RNA-containing particles. Journal of Virology 76 (14), 6919–6928.

Appel, N., Zayas, M., Miller, S., Krijnse-Locker, J., Schaller, T., Friebe, P., Kallis, S., Engel, U., Bartenschlager, R., 2008. Essential role of domain III of nonstructural protein 5A for hepatitis C virus infectious particle assembly. PLoS Pathogens 4 (3), e1000035.

Bartenschlager, R., Penin, F., Lohmann, V., Andre, P., 2011. Assembly of infectious hepatitis C virus particles. Trends in Microbiology 19 (2), 95–103.

Blight, K.J., McKeating, J.A., Rice, C.M., 2002. Highly permissive cell lines for subgenomic and genomic hepatitis C virus RNA replication. Journal of Virology 76 (24), 13001–13014.

Boson, B., Granio, O., Bartenschlager, R., Cosset, F.L., 2011. A concerted action of hepatitis C virus p7 and nonstructural protein 2 regulates core localization at the endoplasmic reticulum and virus assembly. PLoS Pathogens 7 (7), e1002144.

Brohm, C., Steinmann, E., Friesland, M., Lorenz, I.C., Patel, A., Penin, F., Bartenschlager, R., Pietschmann, T., 2009. Characterization of determinants important for hepatitis C virus p7 function in morphogenesis by using trans-complementation. Journal of Virology 83 (22), 11682–11693.

Carrere-Kremer, S., Montpellier-Pala, C., Cocquerel, L., Wychowski, C., Penin, F., Dubuisson, J., 2002. Subcellular localization and topology of the p7 polypeptide of hepatitis C virus. Journal of Virology 76 (8), 3720–3730.

Castelain, S., Bonte, D., Penin, F., Francois, C., Capron, D., Dedeurwaerder, S., Zawadzki, P., Morel, V., Wychowski, C., Duverlie, G., 2007. Hepatitis C Virus p7 membrane protein quasispecies variability in chronically infected patients treated with interferon and ribavirin, with or without amantadine. Journal of Medical Virology 79 (2), 144–154.

Clayton, R.F., Owsianka, A., Aitken, J., Graham, S., Bhella, D., Patel, A.H., 2002. Analysis of antigenicity and topology of E2 glycoprotein present on recombinant hepatitis C virus-like particles. Journal of Virology 76 (15), 7672–7682.

de la Fuente, C., Goodman, Z., Rice, C.M., 2013. Genetic and functional characterization of the N-terminal region of the hepatitis C virus NS2 protein. Journal of Virology 87 (8), 4130–4145.

Delgrange, D., Pillez, A., Castelain, S., Cocquerel, L., Rouille, Y., Dubuisson, J., Wakita, T., Duverlie, G., Wychowski, C., 2007. Robust production of infectious viral particles in Huh-7 cells by introducing mutations in hepatitis C virus structural proteins. Journal of General Virology 88 (Pt 9), 2495–2503.

Dentzer, T.G., Lorenz, I.C., Evans, M.J., Rice, C.M., 2009. Determinants of the hepatitis C virus nonstructural protein 2 protease domain required for production of infectious virus. Journal of Virology 83 (24), 12702–12713.

Di Giorgio, A.M., Hou, Y., Zhao, X., Zhang, B., Lyeth, B.G., Russell, M.J., 2008. Dimethyl sulfoxide provides neuroprotection in a traumatic brain injury model. Restorative Neurology and Neuroscience 26 (6), 501–507.

Dubuisson, J., Hsu, H.H., Cheung, R.C., Greenberg, H.B., Russell, D.G., Rice, C.M., 1994. Formation and intracellular localization of hepatitis C virus envelope glycoprotein complexes expressed by recombinant vaccinia and Sindbis viruses. Journal of Virology 68 (10), 6147–6160.

Gastaminza, P., Kapadia, S.B., Chisari, F.V., 2006. Differential biophysical properties of infectious intracellular and secreted hepatitis C virus particles. Journal of Virology 80 (22), 11074–11081.

Gentzsch, J., Brohm, C., Steinmann, E., Friesland, M., Menzel, N., Vieyres, G., Perin, P.M., Frentzen, A., Kaderali, L., Pietschmann, T., 2013. Hepatitis C Virus p7 is critical for capsid assembly and envelopment. PLoS Pathogens 9 (5), e1003355.

Griffin, S., Stgelais, C., Owsianka, A.M., Patel, A.H., Rowlands, D., Harris, M., 2008. Genotype-dependent sensitivity of hepatitis C virus to inhibitors of the p7 ion channel. Hepatology 48 (6), 1779–1790.

Griffin, S.D., Beales, L.P., Clarke, D.S., Worsfold, O., Evans, S.D., Jaeger, J., Harris, M.P., Rowlands, D.J., 2003. The p7 protein of hepatitis C virus forms an ion channel that is blocked by the antiviral drug, Amantadine. FEBS Letters 535 (1-3), 34–38.

Griffin, S.D., Harvey, R., Clarke, D.S., Barclay, W.S., Harris, M., Rowlands, D.J., 2004. A conserved basic loop in hepatitis C virus p7 protein is required for amantadine-sensitive ion channel activity in mammalian cells but is dispensable for localization to mitochondria. Journal of General Virology 85 (Pt 2), 451–461.

Jirasko, V., Montserret, R., Appel, N., Janvier, A., Eustachi, L., Brohm, C., Steinmann, E., Pietschmann, T., Penin, F., Bartenschlager, R., 2008. Structural and functional characterization of nonstructural protein 2 for its role in hepatitis C virus assembly. Journal of Biological Chemistry 283 (42), 28546–28562.

Jirasko, V., Montserret, R., Lee, J.Y., Gouttenoire, J., Moradpour, D., Penin, F., Bartenschlager, R., 2010. Structural and functional studies of nonstructural protein 2 of the hepatitis C virus reveal its key role as organizer of virion assembly. PLoS Pathogens 6 (12), e1001233.

Jones, C.T., Murray, C.L., Eastman, D.K., Tassello, J., Rice, C.M., 2007. Hepatitis C virus p7 and NS2 proteins are essential for production of infectious virus. Journal of Virology 81 (16), 8374–8383.

Jones, D.M., Atoom, A.M., Zhang, X., Kottilil, S., Russell, R.S., 2011. A genetic interaction between the core and NS3 proteins of hepatitis C virus is essential for production of infectious virus. Journal of Virology 85 (23), 12351–12361.

Jones, D.M., Patel, A.H., Targett-Adams, P., McLauchlan, J., 2009. The hepatitis C virus NS4B protein can trans-complement viral RNA replication and modulates production of infectious virus. Journal of Virology 83 (5), 2163–2177.

Kaul, A., Woerz, I., Meuleman, P., Leroux-Roels, G., Bartenschlager, R., 2007. Cell culture adaptation of hepatitis C virus and in vivo viability of an adapted variant. Journal of Virology 81 (23), 13168–13179.

Lin, C., Lindenbach, B.D., Pragai, B.M., McCourt, D.W., Rice, C.M., 1994. Processing in the hepatitis C virus E2-NS2 region: identification of p7 and two distinct E2-specific products with different C termini. Journal of Virology 68 (8), 5063–5073.

Luik, P., Chew, C., Aittoniemi, J., Chang, J., Wentworth, P.JJr., Dwek, R.A., Biggin, P.C., Venien-Bryan F C., Zitzmann, N., 2009. The 3-dimensional structure of a hepatitis C virus p7 ion channel by electron microscopy. Proceedings of the National Academy of Sciences the United States of America 106 (31), 12712–12716.

Ma, Y., Anantpadma, M., Timpe, J.M., Shanmugam, S., Singh, S.M., Lemon, S.M., Yi, M., 2011. Hepatitis C virus NS2 protein serves as a scaffold for virus assembly by interacting with both structural and nonstructural proteins. Journal of Virology 85 (1), 86–97.

Ma, Y., Yates, J., Liang, Y., Lemon, S.M., Yi, M., 2008. NS3 helicase domains involved in infectious intracellular hepatitis C virus particle assembly. Journal of Virology 82 (15), 7624–7639.

Martins, T., Narciso-Schiavon, J.L., Schiavon Lde, L., 2011. Epidemiology of hepatitis C virus infection. Revista da Associacao Medica Brasileira 57 (1), 107–112.

Masaki, T., Suzuki, R., Murakami, K., Aizaki, H., Ishii, K., Murayama, A., Date, T., Matsuura, Y., Miyamura, T., Wakita, T., Suzuki, T., 2008. Interaction of hepatitis C virus nonstructural protein 5A with core protein is critical for the production of infectious virus particles. Journal of Virology 82 (16), 7964–7976.

McLauchlan, J., 2009. Hepatitis C virus: viral proteins on the move. Biochemical Society Transactions 37 (Pt 5), 986–990.

Meshkat, Z., Audsley, M., Beyer, C., Gowans, E.J., Haqshenas, G., 2009. Reverse genetic analysis of a putative, influenza virus M2 HXXXW-like motif in the p7 protein of hepatitis C virus. Journal of Viral Hepatitis 16 (3), 187–194.

Michaels, A.J., Nelson, D.R., 2010. New therapies in the management of hepatitis C virus. Current Opinion in Gastroenterology 26 (3), 196–201.

Miyanari, Y., Atsuzawa, K., Usuda, N., Watashi, K., Hishiki, T., Zayas, M., Bartenschlager, R., Wakita, T., Hijikata, M., Shimotohno, K., 2007. The lipid droplet is an important organelle for hepatitis C virus production. Nature Cell Biology 9 (9), 1089–1097.

Moradpour, D., Penin, F., Rice, C.M., 2007. Replication of hepatitis C virus. Nature Reviews Microbiology 5 (6), 453–463.

Murray, C.L., Jones, C.T., Rice, C.M., 2008. Architects of assembly: roles of Flaviviridae non-structural proteins in virion morphogenesis. Nature Reviews Microbiology 6 (9), 699–708.

Murray, C.L., Jones, C.T., Tassello, J., Rice, C.M., 2007. Alanine scanning of the hepatitis C virus core protein reveals numerous residues essential for production of infectious virus. Journal of Virology 81 (19), 10220–10231.

Op De Beeck, A., Voisset, C., Bartosch, B., Ciczora, Y., Cocquerel, L., Keck, Z., Foung, S., Cosset, F.L., Dubuisson, J., 2004. Characterization of functional hepatitis C virus envelope glycoproteins. Journal of Virology 78 (6), 2994–3002.

Pavlovic, D., Neville, D.C., Argaud, O., Blumberg, B., Dwek, R.A., Fischer, W.B., Zitzmann, N., 2003. The hepatitis C virus p7 protein forms an ion channel that is inhibited by long-alkyl-chain iminosugar derivatives. Proceedings of the National Academy of Sciences of the United States of America 100 (10), 6104–6108.

Popescu, C.I., Callens, N., Trinel, D., Roingeard, P., Moradpour, D., Descamps, V., Duverlie, G., Penin, F., Heliot, L., Rouille, Y., Dubuisson, J., 2011a. NS2 protein of

hepatitis C virus interacts with structural and non-structural proteins towards virus assembly. PLoS Pathogens 7 (2), e1001278.
Popescu, C.I., Rouille, Y., Dubuisson, J., 2011b. Hepatitis C virus assembly imaging. Viruses 3 (11), 2238–2254.
Premkumar, A., Wilson, L., Ewart, G.D., Gage, P.W., 2004. Cation-selective ion channels formed by p7 of hepatitis C virus are blocked by hexamethylene amiloride. FEBS Letters 557 (1-3), 99–103.
Russell, R.S., Meunier, J.C., Takikawa, S., Faulk, K., Engle, R.E., Bukh, J., Purcell, R.H., Emerson, S.U., 2008. Advantages of a single-cycle production assay to study cell culture-adaptive mutations of hepatitis C virus. Proceedings of the National Academy of Sciences of the United States of America 105 (11), 4370–4375.
Sakai, A., Claire, M.S., Faulk, K., Govindarajan, S., Emerson, S.U., Purcell, R.H., Bukh, J., 2003. The p7 polypeptide of hepatitis C virus is critical for infectivity and contains functionally important genotype-specific sequences. Proceedings of the National Academy of Sciences of the United States of America 100 (20), 11646–11651.
Shepard, C.W., Finelli, L., Alter, M.J., 2005. Global epidemiology of hepatitis C virus infection. Lancet Infectious Diseases 5 (9), 558–567.
Stapleford, K.A., Lindenbach, B.D., 2011. Hepatitis C virus NS2 coordinates virus particle assembly through physical interactions with the E1–E2 glycoprotein and NS3–NS4A enzyme complexes. Journal of Virology 85 (4), 1706–1717.
Steinmann, E., Penin, F., Kallis, S., Patel, A.H., Bartenschlager, R., Pietschmann, T., 2007. Hepatitis C virus p7 protein is crucial for assembly and release of infectious virions. PLoS Pathogens 3 (7), e103.
Tedbury, P., Welbourn, S., Pause, A., King, B., Griffin, S., Harris, M., 2011. The subcellular localization of the hepatitis C virus non-structural protein NS2 is regulated by an ion channel-independent function of the p7 protein. Journal of General Virology 92 (Pt 4), 819–830.
Tellinghuisen, T.L., Evans, M.J., von Hahn, T., You, S., Rice, C.M., 2007. Studying hepatitis C virus: making the best of a bad virus. Journal of Virology 81 (17), 8853–8867.
Vieyres, G., Brohm, C., Friesland, M., Gentzsch, J., Wolk, B., Roingeard, P., Steinmann, E., Pietschmann, T., 2013. Subcellular localization and function of an epitope-tagged p7 viroporin in hepatitis C virus-producing cells. Journal of Virology 87 (3), 1664–1678.
Wang, K., Xie, S., Sun, B., 2011. Viral proteins function as ion channels. Biochimica et Biophysica Acta 1808 (2), 510–515.
Wozniak, A.L., Griffin, S., Rowlands, D., Harris, M., Yi, M., Lemon, S.M., Weinman, S.A., 2010. Intracellular proton conductance of the hepatitis C virus p7 protein and its contribution to infectious virus production. PLoS Pathogens 6 (9), e1001087.
Yi, M., Ma, Y., Yates, J., Lemon, S.M., 2007. Compensatory mutations in E1, p7, NS2, and NS3 enhance yields of cell culture-infectious intergenotypic chimeric hepatitis C virus. Journal of Virology 81 (2), 629–638.
Zhong, J., Gastaminza, P., Cheng, G., Kapadia, S., Kato, T., Burton, D.R., Wieland, S.F., Uprichard, S.L., Wakita, T., Chisari, F.V., 2005. Robust hepatitis C virus infection in vitro. Proceedings of the National Academy of Sciences of the United States of America 102 (26), 9294–9299.
Zhong, J., Gastaminza, P., Chung, J., Stamataki, Z., Isogawa, M., Cheng, G., McKeating, J.A., Chisari, F.V., 2006. Persistent hepatitis C virus infection in vitro: coevolution of virus and host. Journal of Virology 80 (22), 11082–11093.